CHAPTER II
BACKGROUND AND LITERATURE SURVEY

2.1 Crevice Corrosion

Corrosion in narrow gaps is localized corrosion proceeding at a fast rate within a narrow crevice. It ensues from differential aeration. On account of difficulty of oxygen seeping the small cavity, the oxygen concentration is lower in the crevice.

Crevice corrosion may figure out between two adjacent metal pieces or between a metal piece and a nonmetal piece. They may also be simple fractures.

The destruction of crevice may be discussed in more details as shown in Figure 2.1. Here two metal plates are attached with rivets and immersed in water. At site A, in crevice, the contribution of oxygen by diffusion is smaller than at site C, outside the crevice.

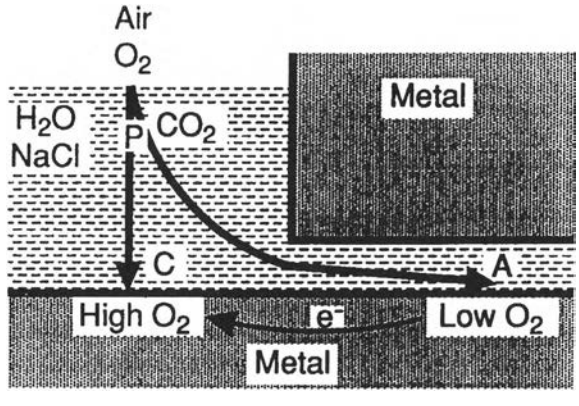

Figure 2.1 Crevice corrosion (Piron, 1991).

Consequently, there is a galvanic cell between site A and site C that sets to cause metal dissolution (e.g.iron), primarily in the crevice that is

$$Fe \longrightarrow Fe^{++} + 2e^-$$

The liberated electrons go to site C, where the reaction with oxygen is dominant and oxygen acts as the likely electron acceptor for liberated electrons.

The surplus of Fe^{++} in the crevice constitutes an excess of positive charges that can react with water, according to the below reaction

$$Fe^{++} + 2H_2O \longrightarrow Fe(OH)_2 + 2H^+$$

This corresponds to the augmentation in acidity observed in the crevice. This lower pH increases the corrosion rate in the crevice. Besides, oxygen is an electron acceptor and has higher availability at site C, it promotes iron dissolution to gain liberated electrons further from site A. Thereby this phenomena also supports the corrosion inside crevice.

2.2 Surface Tension

Surface tension can be viewed into two ways as either the free energy required to create new surface area [energy/(length)^2] or the line of force [forces/length].

Creating a new surface requires work. This work, w, is proportional to the number of molecules transported to the surface and thus to the boundary of the new surface, which can be presented by the basic linear defining equation as

$$w = \gamma \Delta A \qquad (2.1)$$

where γ is called the constant surface tension.

Figure 2.2 shows a simple device consisting of a wire loop with a movable slide that can clarify both ways of viewing surface tension. The device acts as an idealized frictionless apparatus.

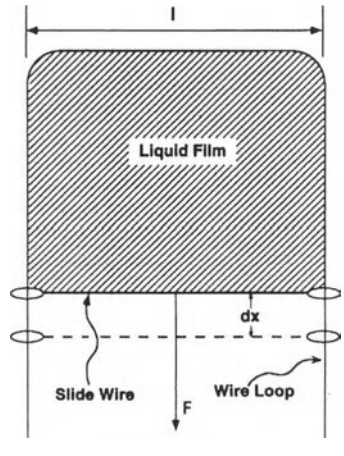

Figure 2.2 Wire loop with a slide wire on which a liquid film can be formed and stretched by an applied force F (Fennell and Wennerstrom, 1994).

The wire loop was dipped into a liquid, forming a liquid film. Surface tension causes the slide wire to move in the direction of decreasing film area unless an opposing force is applied. This force, F, operates along the entire film edge, varies linearly with the length l of the slide wire, and has a characteristic value for each liquid. The apparatus determines the surface tension with the top and bottom surfaces as

$$\gamma = F / 2l \tag{2.2}$$

The work associated with expanding the interfacial area as

$$dw = F\,dx = \gamma\, 2l\, dx = \gamma\, dA \tag{2.3}$$

The work of increasing the area was contributed to the differential Gibbs free energy at constant temperature and pressure which is shown in Equation (2.4)

$$dG = \gamma\, dA \tag{2.4}$$

where

$$\gamma = \left(\frac{\partial G}{\partial A}\right)_{T,P} \tag{2.5}$$

This expression shows surface tension as the increase in Gibbs free energy per unit area increased.

2.3 The Work of Adhesion and Cohesion

The concepts of adhesion and cohesion was needed to clarify how liquids behave when they come into contact. In a single liquid, the work of cohesion corresponds to the work required to pull apart a volume of unit cross-sectional area, as shown in Figure 2.3 and the equation

$$\Delta G = w_{AA} = 2\gamma_{\alpha} \tag{2.6}$$

(sometimes a surface tension γ_{α} was denoted as $\gamma_{\alpha v}$ to describe that the second phase is a vapor).

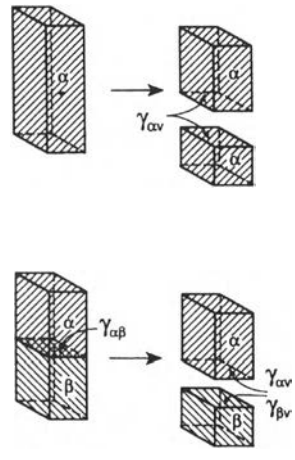

Figure 2.3 (a) The work of cohesion, $w_{AA} = 2\gamma_{\alpha v}$, in a liquid, (b) The work of adhesion, $w_{AB} = \gamma_{\alpha v} + \gamma_{\beta v} - \gamma_{\alpha\beta}$, to separate the unit area of the interface into two liquid-air interfaces (Fennell and Wennerstrom, 1994).

Presenting $\gamma_{\alpha v}$ as half of the cohesion work indicates that surface tension measures the free energy change included when molecules from the bulk of a sample are moved to its surface.

Having two interfaces /surfaces is clearly advantageous if sum of free energies of the two surfaces, $\gamma_{sl} + \gamma_{lv}$, is smaller than free energy of the initial surface γ_{sv}. Therefore, it is natural to introduce a spreading coefficient, S.

$$S = \gamma_{sv} - (\gamma_{sl} + \gamma_{lv}) \qquad (2.7)$$

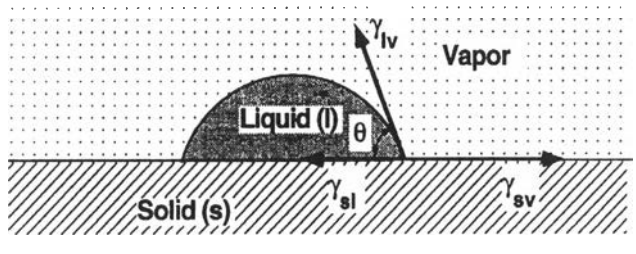

Figure 2.4 Contact angle on a solid surface (Fennell and Wennerstrom, 1994).

When S $\geq$ 0, spreading will take place, while for negative S, the liquid forms a finite lens.

From Equations (2.6) and (2.7), the spreading coefficient is related to the work of adhesion and cohesion as shown in the below equation

$$S = w_{AB} - 2\gamma_A = w_{AB} - w_{AA} \quad (2.8)$$

2.4 Capillary Rise in a Cylinder

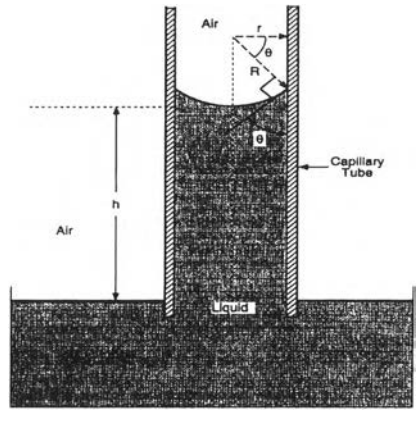

Figure 2.5 A schematic diagram of the capillary rise.

The phenomenon of capillary rise, which is attributed to be one of the most accurate methods, can be used to determine the surface tension of a liquid. In the capillary tube, the liquid surface curve is a spherical cap as shown in the Figure 2.5. A capillary tube is dipped into a liquid that wets the tube. The liquid rises in a capillary by means of capillary force and force of wetting between the liquid and the tube.

Factors on which the height of the rising liquid depend include the radius of the capillary radius r, the surface tension of the liquid γ, and the contact angle θ, between the tube wall, the air, and the liquid. The equation that has been widely used to treat such the phenomenon is

$$\gamma = \frac{\rho g H r}{2\cos\theta} \quad (2.9)$$

This equation is particularly simple to apply when the liquid wets the solid surface so that $\cos\theta = 1$. In this case it suffices to know ρ, r, and measure h to be able to calculate the liquid-vapor surface tension, γ.

2.5 The Laplace Equation

Surface tension operates in a liquid film, and, to obtain mechanical equilibrium, this tension must be balanced by some equal and opposite force. For example, to blow a bubble in a liquid medium, an excess pressure is applied. In an isolated particle, such as a droplet, the balancing force comes from stresses within the particle.

The insight that is central to this development is that a pressure difference operates across a curved interface. The pressure difference is such that the greater pressure is on the concave side. Our objective in this section is to relate this pressure difference to the curvature of the surface.

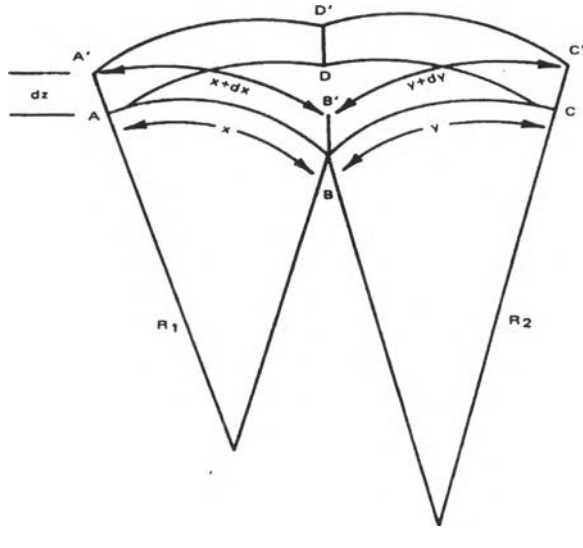

Figure 2.6 Definition of coordinates describing the displacement of an element of curved surface ABCD to A′B′C′D′ (Hiemenz, 1986).

Figure 2.6 shows a part ABCD of a curved surface. The surface has been cleaved by two planes which are perpendicular to one another. Each of the planes therefore contains a portion of arc where it intersects the curved surface. In the figure the radii of curvature are designated R_1 and R_2, and the lengths are designated x and y, respectively, for these two intercepted arcs. The curvature of a surface, at a point, is described in terms of the radii R_1 and R_2 of the curves corresponding to that point.

The curved surface is moved outwardly by a small amount dz to a new position that is A′B′C′D′. Since the corners of the surface continue to lie along extensions of the diverging radial lines, this move increases the arc lengths to $x + dx$ and $y + dy$. Obviously the area of surface must also increase. The work required to accomplish this must be supplied by a pressure differrence Δp across the element of surface area.

The area expansion when the surface is displaced is given by

$$dA = (x + dx)(y + dy) - xy = x\,dy + y\,dx + dx\,dy \approx x\,dy + y\,dx \quad (2.10)$$

where the approximation arises from neglecting second-order differential quantities. The increase in free energy associated with this increase in area is given by $\gamma\,dA$:

$$dG = \gamma\,(x\,dy + y\,dx) \quad (2.11)$$

If the expansion of this surface is responsible with ordinary pressure-volume work, then the work equals $\Delta p\,dV$, where dV is the volume swept by the moving surface. In terms of Figure 2.6, this equals

$$dw = \Delta pxy\,dz \quad (2.12)$$

Equations (2.11) and (2.12) are equal then they are rearranged to get the below Equation (2.13)

$$\gamma\,(x\,dy + y\,dx) = \Delta pxy\,dz \quad (2.13)$$

From similar triangles application, we may establish the following proportions from Figure 2.6, there are

$$\frac{x + dx}{R_1 + dz} = \frac{x}{R_1} \quad (2.14)$$

and

$$\frac{y + dy}{R_2 + dz} = \frac{y}{R_2} \quad (2.15)$$

which can be simplified to

$$\frac{dx}{xdz} = \frac{1}{R_1} \tag{2.16}$$

and

$$\frac{dy}{ydz} = \frac{1}{R_2} \tag{2.17}$$

Substituting Equations (2.16) and (2.17) into Equation (2.13) enables us to write the relationship of Δp to R_1, R_2 and γ as follows

$$\Delta p = \gamma \left(\frac{1}{R_1} + \frac{1}{R_2} \right) \tag{2.18}$$

This expression was derived in 1805 and is known as the Laplace equation.

Since this is the case, Equation (2.18) is general and applies equally well to geometrical bodies whose radii of curvature are constant over the entire surface or to more intricate shapes where the radii of curvature change from place to place on the surface. For the former category there are several special cases of Equation (2.18) that are worthy of note:

1. For a sphere, $R_1 = R_2 = R$, therefore

$$\Delta p = \frac{2\gamma}{R} \tag{2.19}$$

2. For a cylinder, $R_1 = R$ and $R_2 = \infty$, therefore

$$\Delta p = \frac{\gamma}{R} \tag{2.20}$$

3. While for a plane, $R_1 = R_2 = \infty$, therefore

$$\Delta p = 0 \tag{2.21}$$

The curved surface under consideration, which is also possible for a portion of a surface to be locally saddle shaped, the two radii of curvature lie on opposite sides of the surface and have different signs. It is possible for p to be zero in this situation also.

Physically, the Equation (2.18) indicates that interfacial tension causes an increased pressure on the inside of the surface, the radii of curvature of the surface have an effect on the magnitude of that pressure. It also shows that there is a

corresponding discontinuity in normal stress, which acts perpendicular to the surface, across the boundary.

2.6 Numerical Solution of Differential Equations by Euler's Method

The numerical technique can readily be adapted to the solution of more complicated differential equations, and whose analytical solution is either difficult or impossible. This section is devoted to solve ordinary differential equations of the form

$$\frac{dh}{dr} = f(h, r)$$

where $f(h, r)$ is the differential equation evaluated at h and r. This estimation can be done at any time along the way of

New value = old value + slope × step size

Or, in mathematical terms,

$$h_{i+1} = h_i + \phi(\Delta r) \tag{2.22}$$

According to this equation, the slope estimate of ϕ is used to extrapolate from an old value h_i to a new value h_{i+1} over a distance Δr.(Note that this approach is formally called *Euler's method.*)

2.7 Literature Survey

Grzybowski *et al.* (2001) examined lateral capillary interactions between millimeter and sub-millimeter-sized objects floating at the interface of perfluorodecalin (PFD) and water. Analytical solutions of the Laplace equation were obtained for two infinitely long faces in terms of the meniscus height and the distance between plate to plate. The relations were also used to calculate the energy of the system by sum of the capillary and gravitational energy terms. Moreover, they used Finite Element Method to model the contours of the menisci. They suggested that the Finite Element Method is a reliable tool for imaging and studying menisci, and of studying capillary interactions between objects.

A new technique to determine interfacial tension was proposed by Lee *et al.* (2001). Micropipet has been developed to measure the equilibrium and dynamic interfacial tensions of microscopic liquid-gas and liquid-liquid interfaces that were determined by measuring the radius of curvature of the interface for a series of pressure changes on the basis of the Laplace equation. While assuming the contact angle was zero, their results were consistent with the interfacial tension values reported in the literature determined by other techniques for microscopic interfaces.

Hahm *et al.* (2000) presented a novel and simple method for preparing micron-scale annular structures formed from polystyrene-*b*-poly(methyl methacrylate) diblock copolymer films on the silicon oxide substrates via prewetting of the underlying substrate with a minor polar solvent before spin-casting of diblock solution. The cylinder-forming microdomains of PS-*b*-PMMA annuli exposed the unique alignment without the aid of an external alignment field. These aligned microdomains was controlled in nanometer-scale spacing and coherence on the order of microns.

Chatelier *et al.* (1997) used the theoretical approach to model the equilibrium capillary height (h_{eq}) of electrolyte solution between ionizable surfaces on flat plates as a function of pH. Their results showed that the dependence of h_{eq} on pH depends on the number of ionizable surface sites per unit area, the intrinsic acid-base dissociation constant (K_a^i) of the surface sites, and the background electrolyte. Reasonable best-fit values were obtained for the surface density and the intrinsic pK_a of the ionizable groups.